Modelling of the Micro-Mechanical Behaviour of Steel Sheets During Deep-Drawing

L. Duchêne, A. Godinas, A. M. Habraken, S. Cescotto
University of Liège, Belgium

Abstract

This paper presents a constitutive law based on Taylor's model implemented in our non-linear finite element code LAGAMINE. The yield locus is only locally described and a particular interpolation method has been developed. This local yield locus model uses a discrete representation of the material's texture. The interpolation method is presented and a deep-drawing application is simulated in order to show up the influence of the texture evolution during forming processes.

Keywords: Texture evolution, yield locus, finite elements, deep-drawing

1 State of the Problem

The objective of our research is to integrate the influence of the material's texture into a finite element code. The constitutive law describing the mechanical behaviour of the studied sample is based on a microscopic approach. The law computation takes place on the crystallographic level. A large number of crystals must be used to represent correctly the global behaviour. The micro-macro transition links the global behaviour to the crystallographic results. The full constraint Taylor's model is used for the computation of the microscopic behaviour of each crystal and for the micro-macro transition. Unfortunately, this model does not lead to a general law with a mathematical formulation of the yield locus. Only one point of the yield locus corresponding to a particular strain rate direction can be computed.

The "direct Taylor's model" assumes that one macroscopic stress results from the average of the microscopic stresses related to each crystal belonging to a set of representative crystals. The computation of the mechanical behaviour involves a large number of crystals and must be repeated for each integration point of the finite element model, for each iteration of each time step. So, such a micro-macro approach consumes large computation time and seems practically not usable.

However, using different simplified approaches, various constitutive laws based on texture analysis have been implemented in the non-linear finite element code LAGAMINE. Our first step in the integration of the texture effects has been the use of a 6^{th} order series yield locus defined by a least square fitting on a large number of points (typically 70300) in the deviatoric stress space (see [3]). Those points were calculated by Taylor's model based on an assumed constant texture of the material. This fitting is performed once, outside the FEM code.

It provides 210 coefficients to describe the whole yield locus. This method, i.e. a global description of the yield locus, is actually used in the FEM code.

Unfortunately, taking into account the texture evolution effects with this yield locus would imply the computation of the 210 coefficients of the 6^{th} order series for each integration point, each time a texture updating is necessary. This would require an impressive amount of computation and memory storage (210 coefficients for each integration point) which is only partially useful as generally the stress state remains in a local zone of the yield locus. So, two new approaches, where the whole yield locus is unknown, have been investigated.

In the first case, some points in the interesting part of the yield locus are computed with Taylor's model. This local zone of the yield locus is then represented by a set of hyperplanes, which are planes defined in the five-dimensional deviatoric stress space. These planes being fitted on Taylor's points.

As it has been shown in [1], the yield locus discontinuities bred by this very simple interpolation method give rise to convergence problems in the finite element code. That is the reason why a second method has been developed.

For that second approach, no yield locus is defined and a direct stress-strain interpolation between Taylor's points is achieved. In this case, the yield stress continuity conditions are fulfilled but, as there is no yield locus formulation, a particular stress integration scheme has to be used.

Both interpolation methods allow us an important computation time reduction with respect to the "direct Taylor's model" application. Taylor's model is only used to compute some points in order to achieve the interpolation.

These points must be computed in two cases:

- When the current part of the yield locus does not content anymore the new stress state and that a new local zone of the yield locus is required.
- When the plastic strains significantly deform the material and induce changes in the crystallographic orientations, i.e. when the texture evolves. Indeed, the corresponding mechanical behaviour of the material would no more be correctly represented by the old points. A texture updating must take place.

The part yield locus approach presented in this paper can be placed between the microscopic approach (accurate but very slow) and the global yield locus approach (fast but inaccurate and especially not adapted for texture updating).

This paper describes the stress-strain interpolation method; interested readers can refer to [1], [2], [3] and [5] for the 6^{th} order and the hyperplanes method. The influence of the texture updating during a forming process has been highlighted by a deep-drawing simulation.

2 Stress-Strain Interpolation

2.1 Local description of a scaled yield locus.

This model is particular in the sense that it does not use a yield locus formulation neither for the interpolation nor in the stress integration scheme.

We use a linear stress-strain interpolation described by Equation 1.

$$\underline{\sigma} = \tau \cdot \underline{\underline{C}} \bullet \underline{u} \tag{1}$$

In this equation, $\underline{\sigma}$ is a 5-D vector containing the deviatoric part of the stress; the hydrostatic part being elastically computed according to Hooke's law. The 5-D vector $\underline{u}$ is the deviatoric plastic strain rate direction; it is a unit vector. τ is a scalar describing the work hardening according to the exponential relationship of Equation 2 where the strength coefficient K, the offset Γ^0 and the hardening exponent n are material parameters fitted to experimental data and Γ is the polycrystal induced slip.

$$\tau = K \cdot \left(\Gamma^0 + \Gamma\right)^n \tag{2}$$

The interpolation is included in the matrix $\underline{\underline{C}}$ of Equation 1 and is based on the following concepts. We assume 5 directions: $\underline{u}_i$ (i=1...5) advisedly chosen in the deviatoric strain rate space and the associated deviatoric stress: $\underline{\sigma}_i$ (i=1...5) lying on the yield surface according to the Taylor's model. These points will define the interpolation domain and will be called stress nodes. Additionally, we compute the contravariant vectors $\underline{ss}_i$ and $\underline{uu}_i$ defined by Equations 3 and 4.

$$\underline{ss}_i \bullet \underline{\sigma}_j = \delta_{ij} \tag{3}$$

$$\underline{uu}_i \bullet \underline{u}_j = \delta_{ij} \tag{4}$$

With the use of those contravariant vectors we define intrinsic co-ordinates in the interpolation domain for any stress vector $\underline{\sigma}^*$ by projection according to Equation 5 and for any plastic strain rate direction $\underline{u}^*$ with Equation 6.

$$\eta_i = \underline{\sigma}^* \bullet \underline{ss}_i \tag{5}$$

$$\eta_i = \underline{u}^* \bullet \underline{uu}_i \tag{6}$$

The most important property of our stress-strain interpolation states that if the stress $\underline{\sigma}^*$ and the plastic strain rate direction $\underline{u}^*$ physically correspond to the same point, then the intrinsic co-ordinates η_i computed for $\underline{\sigma}^*$ (Equation 5) or for $\underline{u}^*$ (Equation 6) are equal.

The interpolation is achieved with the use of those intrinsic co-ordinates to compute the stress or the strain rate with a common formulation:

$$\underline{\sigma} = \sum_i \eta_i \cdot \underline{\sigma}_i \tag{7}$$

$$\underline{u} = \sum_i \eta_i \cdot \underline{u}_i \tag{8}$$

Putting together Equations 6 and 7, we can compute the stress associated to a plastic strain rate direction and get the expression of the interpolation matrix $\underline{\underline{C}}$ (the hardening not being taken into account here):

$$\underline{\sigma} = \underbrace{\sum_i \underline{\sigma}_i \cdot \underline{uu}_i}_{=\underline{\underline{C}}} \bullet \underline{u} \tag{9}$$

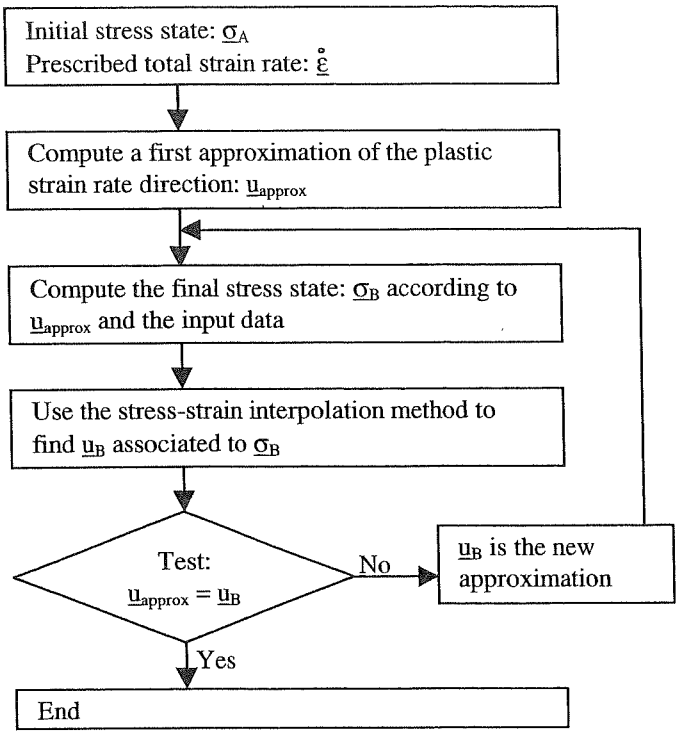

Figure 1: *Stress integration scheme*

As long as the interpolation is achieved in the domain delimited by the 5 stress nodes, all the 5 η_i must remain between 0 and 1. When one of the 5 η_i becomes negative, it means that the current stress is out of the domain and an updating of the stress nodes must take place. The classical updating method consists in finding 5 new stress nodes defining a new domain containing the current stress direction. The developed improved updating method makes use of the adjacent domain. Therefore, only 1 new stress node is computed with the Taylor's model and 4 of the 5 old stress nodes are kept for the interpolation. The main advantages of this method are that it requires only 1 (instead of 5) Taylor's model call for an updating and it improves the continuity of the resulting yield locus and the continuity of its normal.

2.2 Stress integration scheme

As already mentioned, the stress-strain interpolation relation (Equation 1) does not use the concept of yield locus in a classical way. So, a specific integration scheme has been developed. The stress integration scheme implemented with our interpolation method is completely different from the classical radial return with elastic predictor; the main ideas are summarised in the diagram of Fig. 1 where obviously, no yield locus formulation is used.

As it has been observed during several finite element simulations, this stress integration scheme is well adapted for a local yield locus description and induces a reasonable number of interpolation domain updating.

2.3 Implementation of the texture updating

The principal characteristic of our texture updating model is that it is based on the application of the Taylor's assumptions with a full constraint method on a discrete set of orientations

representing the material's texture (computed according to [4]). It should be pointed out that the constitutive law is based on the interpolation method described earlier and on the Taylor's model applied on the actual set of crystallographic orientations. These orientations are represented with the help of the Euler angles ranging from 0° to 360° for φ_1 and from 0° to 90° for ϕ and φ_2 so as to take crystal cubic symmetry into account but not the sample symmetry. In the code, a loop on the elements especially dedicated to texture evolution has been added in order to achieve the orientation set updating only after time step convergence. The lattice rotation of each crystal is computed with the same Taylor's model by subtracting the slip induced rotation from the rigid body rotation included in the strain history.

3 Deep-Drawing Simulations

In order to show up the influence of the texture evolution during a forming process, a deep-drawing simulation has been examined. Three steels are compared according to their behaviour during the process. The first one is a mild steel, the second one is a dual phase steel and the third one is a complex phase steel. During the calibration of the mechanical properties of these steels which was achieved through tensile tests, extremely different behaviours have been noticed. Their hardening exponents are respectively 0.2186, 0.2238 and 0.1397. Moreover their tensile yield stresses are 136, 293 and 741 N/mm^2 (a factor larger than 5 between them). As we focus on the texture of these steels, their Orientation Distribution Function (ODF) has been measured by X-ray diffraction. The maximum value of this function, i.e. the density of the most represented crystallographic orientation (see Tab. 1) is an indication of the anisotropy of the studied material.

For this application, the behaviour of the material and particularly its texture have been integrated in the code through a constitutive law based on the 6th order series (see [3] and [5]).

Now, the geometry of the deep-drawing process should be presented. A hemispherical punch with a diameter of 100 mm, a die with a curvature radius of 5 mm and a blankholder are the drawing tools. The drawing ratio is 1.7; the blankholder force is 70 kN; the simulation is achieved up to a drawing depth of 50 mm. This geometry has already been used as the benchmark for the NUMISHEET'99 conference. A Coulomb law is used to model the friction with a coefficient adapted to each steel.

On the finite element mesh, a particular element chosen such that it undergoes completely the drawing process on the curvature of the die is examined. The texture evolution of that element is compared for the three steels. The values of the maximum of the ODF for each steel before and after the process are summarised in Tab. 1.

Table 1: *Maximum value of the ODF during deep-drawing*

Steel	*Before deep-drawing*	*After*
Mild steel	6	14.34
Dual phase steel	4.12	6.73
Complex phase steel	6.94	8.52

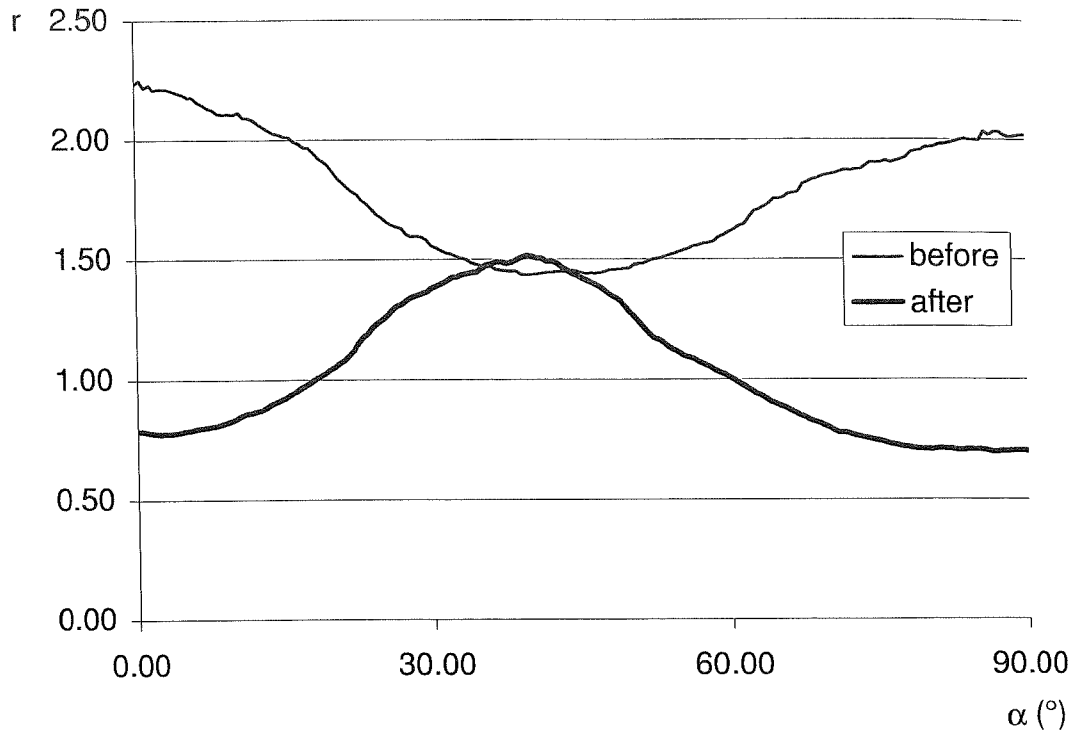

Figure 2: *Evolution of the Lankford coefficient for the mild steel before and after deep-drawing (α is the angle from the Rolling Direction)*

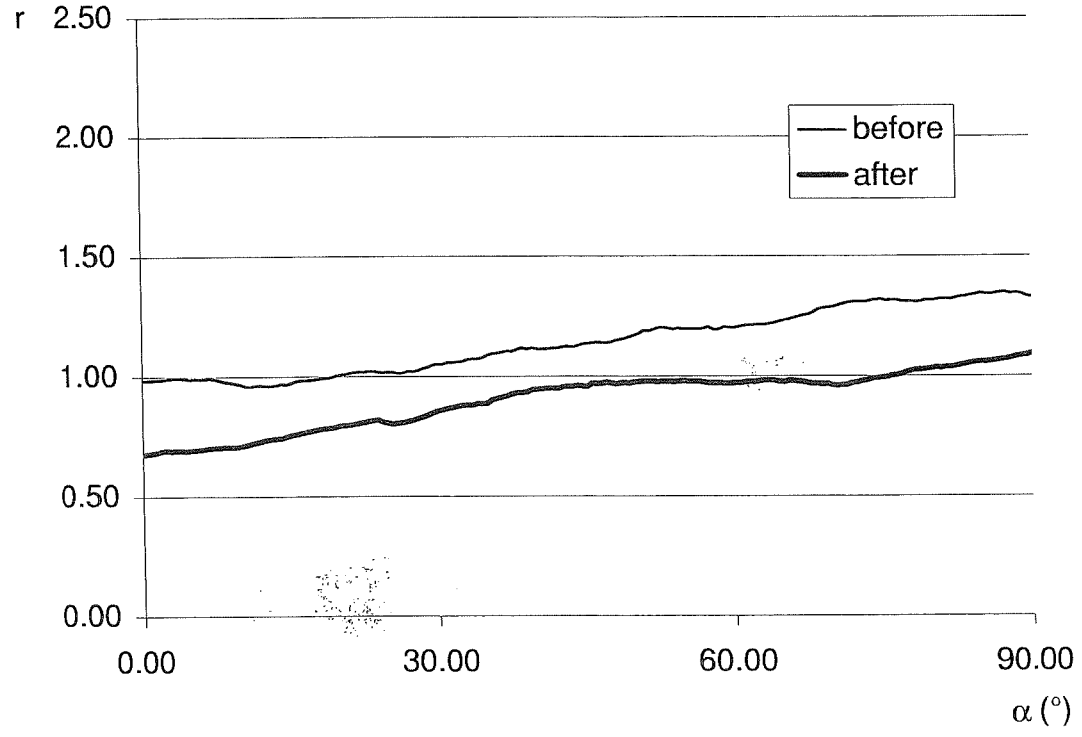

Figure 3: *Evolution of r coefficient for the dual phase steel*

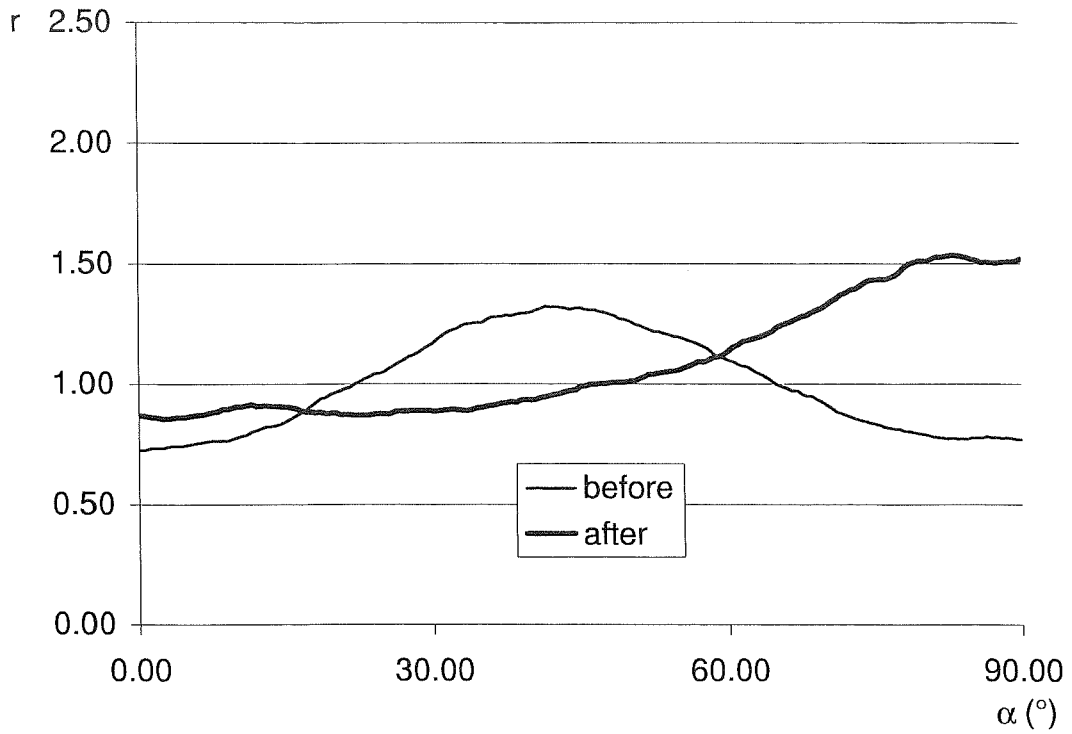

Figure 4: Evolution of r coefficient for the complex phase steel

From Tab. 1, it can be noticed that the initial anisotropy of the three steels is more or less the same. On the other hand, the behaviour of these steels is quite different during deep-drawing if we focus on the maximum of the ODF (a factor larger than 2 is found at the end of the forming process).

These differences in the steel behaviour can also be pointed out with the use of the Lankford coefficients (r). It is indeed interesting to look at the evolution of the Lankford coefficients during deep-drawing as this parameter is a good indicator for the ability of a steel for deep-drawing (a high value of r allows larger deep-drawing ratios).

Fig. 2, 3, 4 show the evolution of the Lankford coefficients during the deep-drawing process. Here again, large differences between the three steels can be noticed. The mild steel is characterised by a high initial r coefficient (inducing a good formability) and a considerable evolution during the simulation. The two other steels have a lower value (around 1.0) and their evolution is also lower. These behaviours are in agreement with the conclusion drawn from the evolution of the maximum of the ODF (see Tab. 1).

4 Conclusions

On the deep-drawing application presented here, large texture evolutions have been noticed. Depending on the steel, these evolutions result in modification of the Lankford coefficients. Finally, the behaviour of the steel sheet during a forming process can be quite different from the initial steel characteristics.

As its texture evolution is the most important, the mild steel simulations are used to validate our approach. Different constitutive laws neglecting or not the texture updating are

applied and the results will be compared to experimental measurements. This validation step is currently going on.

5 References

[1] L. Duchêne, A. Godinas and A. M. Habraken, *Metal plastic behaviour linked to texture analysis and FEM method*, Proc. 4th Int. Conf.: NUMISHEET'99.

[2] L. Duchêne, A. M. Habraken and S. Cescotto, *Elastoplastic anisotropic model based on texture analysis to simulate steel sheet behavior*, Proc. 7th Int. Symp., Cancun, Mexico, 1999.

[3] S. Munhoven, A. M. Habraken, A. Van Bael and J. Winters, *Anisotropic finite element analysis based on texture*, Proc. 3rd Int. Conf.: NUMISHEET'96, pp 112-119.

[4] L. S. Toth and P. Van Houtte, *Discretization techniques for orientation distribution function*, Textures and Microstructures, Vol. 19, 1992, pp 229-244.

[5] J. Winters, *Implementation of Texture-Based Yield Locus into an Elastoplastic Finite Element Code*, Ph. D. Thesis, KUL, Leuven, 1996.